Eur. Phys. J. B **14**, 29–42 (2000)

THE EUROPEAN PHYSICAL JOURNAL B

EDP Sciences

Anisotropic magnetic exchange in orthorhombic RCu_2 compounds (R = rare earth)

M. Rotter[1,a], M. Loewenhaupt[2], S. Kramp[2,5], T. Reif[3], N.M. Pyka[4], W. Schmidt[5], and R. van de Kamp[6]

[1] Institut für Experimentalphysik, Technische Universität Wien, Wiedner Hauptstraße 8–10, 1040 Wien, Austria
[2] Institut für Angewandte Physik, Technische Universität Dresden, 01062 Dresden, Germany
[3] Institut für Festkörperforschung, Forschungszentrum Jülich, 52425 Jülich, Germany
[4] TU München, Zentrale Betriebseinheit FRM - II, 85747 Garching, Germany
[5] Institut Laue Langevin, BP 156 38042 Grenoble Cedex 9, France
[6] Hahn Meitner Institut, 14109 Berlin, Germany

Received 21 April 1999

Abstract. The magnetic excitations in the field induced ferromagnetic phase F3 of a $NdCu_2$ single crystal were investigated by means of inelastic neutron scattering experiments. A mean field model using the random phase approximation in connection with anisotropic magnetic bilinear R-R (R denotes a rare earth) exchange interactions is proposed to account for the observed dispersion. The relevance of this model to the analysis of the magnetic ordering process in other RCu_2 compounds is discussed.

PACS. 75.30.Et Exchange and superexchange interactions

1 Introduction

The magnetic structures of $NdCu_2$ in zero field and for magnetic fields parallel to the b axis of the orthorhombic crystal have been the topic of extensive studies [1–3]. For the corresponding magnetic phase diagram and the description of the different magnetic phases we refer the reader to the given references. The investigation of the magnetic excitations is an important dynamical counterpart to the determination of the static magnetic structure, leading to conclusions about the magnetic ground state and the detailed form of the magnetic interactions. By measuring the field and temperature dependence of the magnetic excitations it is possible to refine theoretical models for the magnetic ordering process.

In $NdCu_2$ the zero field phase AF1 consists of a complicated stacking of 10 ferromagnetic bc planes in a direction leading to an excitation spectrum with 20 branches within an energy range from 0.6 to 2.0 meV [4,5]. The presently available resolution of neutron spectrometry, however, is not sufficient to determine all branches unambiguously unless detailed theoretical predictions are available. For these reasons the magnetic excitations have been measured in the field induced ferromagnetic state, where only two branches appear that can be easily resolved by experiment and that can be calculated very fast by an analytical formula that can be used for a fit.

The paper is organized in the following way: In the first section the details of the neutron scattering experiments will be described, then the results are presented followed by a discussion of the symmetry of the magnetic interactions and an outline of the method used to calculate the magnetic excitations. A quantitative analysis of the experimental data is performed, followed by a discussion about its relevance to other RCu_2 compounds in the final section of the paper.

[a] e-mail: martin_rotter@hotmail.com

2 Experiments

The inelastic neutron scattering (INS) experiments have been performed on a large $NdCu_2$ single crystal ($5 \times 7.5 \times 5.2$ mm^3) that was also used for the magnetic structure determination and is described elsewhere [2]. The majority of the INS measurements was carried out on the IN12 triple-axis spectrometer at the Institut Laue-Langevin, Grenoble, using vertical and horizontal magnetic fields of 3 T. Additional experiments have been performed on the V2 triple-axis spectrometer at the BER2-reactor of the Hahn-Meitner-Institut, Berlin, equipped with a horizontal cryomagnet operated at 3 Tesla. Monochromator and analyzer of both spectrometers were made of pyrolytic-graphite (002) crystals. The IN12 spectrometer has been run in constant-momentum-transfer (constant-$\mathbf{Q}$) mode with variable incident-neutron energy, bent monochromator and flat analyzer. No filter has been used because higher order contaminations are filtered out by the bent neutron guide. When working with vertical magnetic field ((010)-scattering plane) the scattered-neutron

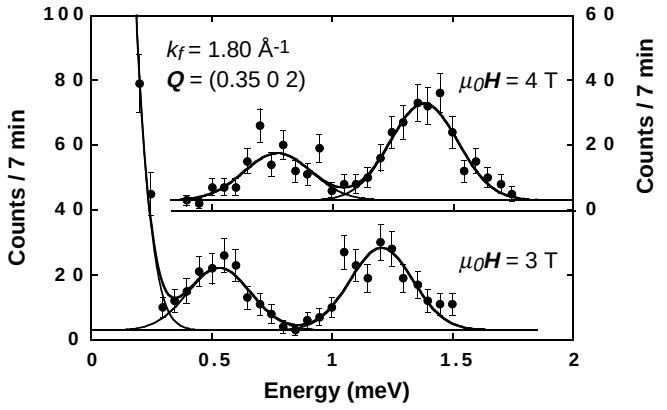

Fig. 1. Magnetic excitations of $NdCu_2$ for $\mathbf{Q}$ = (0.35 0 2). At this wave vector the minimal energy of the dispersion was measured. The upper scan shows the shift of the magnetic excitations when increasing the applied magnetic field.

energy was kept fixed at $k_f = 1.8$ Å^{-1} (6.7 meV). In horizontal field ((001)-scattering plane) the final neutron energy has been varied between $k_f = 1.7$ Å^{-1} (6.0 meV) and 2.1 Å^{-1} (9.2 meV) in order to get access to some $\mathbf{Q}$-vectors in (h00)-direction. This variation was necessary because of geometrical restrictions due to the construction principle of the horizontal cryomagnet. Nevertheless, only a few points near the zone boundary could be measured in (h10)-direction on IN12. The study of the (h00)-direction could be completed at the V2 spectrometer using a new horizontal cryomagnet with only two, relatively small blind spots. This experiment was carried out in constant-$\mathbf{Q}$ mode with fixed scattered-neutron energies of $k_f = 1.1$ Å^{-1} (2.5 meV), 1.4 Å^{-1} (4.1 meV) and 1.55 Å^{-1} (5.0 meV). A cooled Be-filter was placed in front of the analyzer. Monochromator and analyzer have been used in focusing geometry.

3 Results

The measurements have been carried out along the principle symmetry directions (h00), (0k0) and (00l) at T = 1.8 K and B = 3 T. Under these conditions the lattice parameters have been determined to $a = 4.385$ Å, $b = 6.997$ Å and $c = 7.385$ Å. Due to the two Nd^{3+} ions per unit cell in the ferromagnetically ordered phase two magnon branches are expected from the crystal field (CF) ground state doublet. With magnon energies < 2 meV these excitations are well separated from transitions to the higher CF-levels [6].

As an example, Figure 1 shows a constant-$\mathbf{Q}$ spectrum at the reciprocal lattice vector $\mathbf{Q}$ = (0.35 0 2). The two excitations with energies 0.53 meV and 1.21 meV are clearly separated. The magnetic origin of the measured excitations has been checked by increasing the magnetic field from 3 T to 4 T. Due to the Zeeman contribution the energy of the two excitations shifts by about 0.2 meV to 0.77 and 1.38 meV (see Fig. 1). Energy scans at other

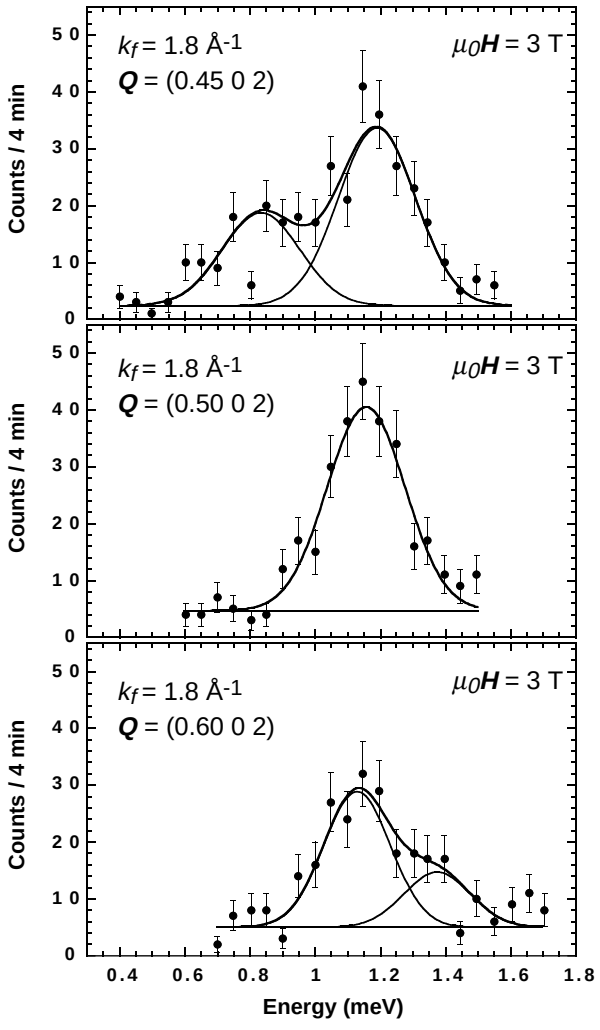

Fig. 2. Constant $\mathbf{Q}$ scans along (h 0 2) showing the crossing of the two modes at (0.5 0 2).

points along the symmetry directions of the reciprocal lattice revealed, that the scan shown in Figure 1 corresponds to an absolute minimum of the dispersion. Note that the position of the spin wave minimum does not coincide with the ordering wave vector $\boldsymbol{\tau}$ = (0.6 0 0) of the antiferromagnetic zero-field phase AF1.

Three subsequent scans along the (h 0 2) direction are shown in Figure 2. At $\mathbf{Q}$ = (0.45 0 2) the lower excitation has moved up to 0.83 meV, whereas the upper did not change. The scans at (0.5 0 2) and (0.6 0 2) indicate, that a stronger, nondispersive mode at about 1 meV is crossed by a weak, dispersive mode at (0.5 0 2).

Energy scans performed along (h 0 1) revealed only one, weakly dispersive branch above 1 meV. It is the same branch, which is observable along (h 0 2), but there the second branch appears as well.

To investigate the behavior of the two modes separately, scattering experiments in the ab plane were performed at the V2 spectrometer using a new horizontal cryomagnet with large accessible angular range. For $\mathbf{Q}$ in the reciprocal ab plane only one excitation can be

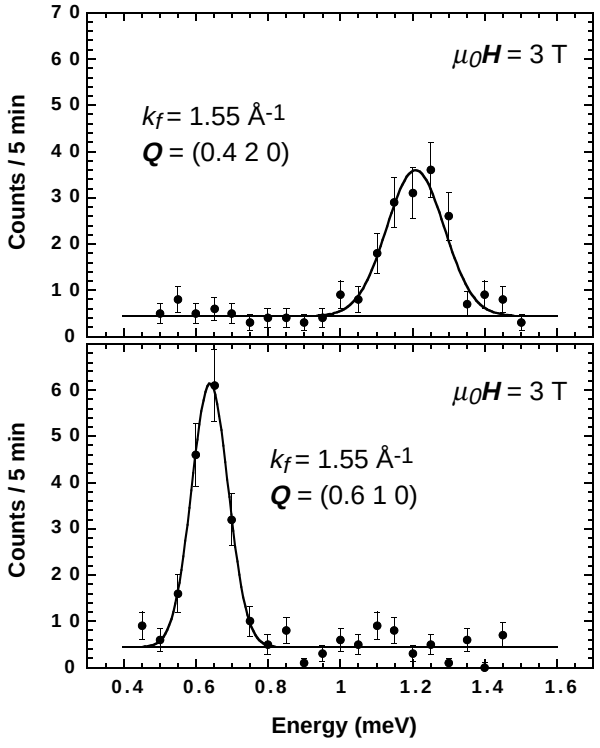

Fig. 3. Constant **Q** scans at two equivalent positions in the reciprocal *ab* plane of $NdCu_2$ measured in the horizontal field configuration. Only one excitation may be observed under these conditions (see text).

measured, because the second excitation has no intensity due to the structure factor. This property is due to the fact, that the projection of the $CeCu_2$ – type structure into the *ab* plane can be described by a primitive rectangular two dimensional lattice. Figure 3 exemplifies this situation at the two equivalent positions (0.4 2 0) and (0.6 1 0). It is instructive to compare the two excitations observed along (h 0 2) to equivalent points along (h 1 0) and (h 2 0): along (h 1 0) the strongly dispersive mode can be measured, whereas along (h 2 0) only the weakly dispersive excitation can be observed.

Unfortunately, even with the new horizontal cryomagnet on the V2 spectrometer not all **q** values were accessible ($\mathbf{q} = \mathbf{Q} - \boldsymbol{\tau}$ with $\boldsymbol{\tau}$ being a reciprocal lattice vector). However, the dispersive branch could clearly be followed from the zone boundary at (0 1 0) up to (0.6 1 0). Crossings of the two modes have been found at $\mathbf{q}$ = (0.2 0 0) and $\mathbf{q}$ = (0.53 0 0).

The results of all scans performed along the symmetry directions of the reciprocal lattice are summarized in Figure 7 and will be discussed in comparison with the calculated dispersion in Section 5. The energies of the two modes at the Γ point have been determined at (0 0 2) to 1.18 meV and 1.63 meV.

4 The MF-RPA model for magnetic excitations

For the calculation of the magnetic excitations in systems with low symmetry great care has to be taken about the anisotropy of the magnetic interactions. In general there are several sources of magnetic anisotropy: single ion and two ions, the most investigated being single ion anisotropy originating from crystal fields. The two ions anisotropy is often considered to be of minor importance and therefore neglected, *i.e.* an isotropic Heisenberg type of magnetic exchange is assumed, especially for high symmetry compounds where anisotropic exchange constants are partly zero for reason of symmetry.

In the orthorhombic RCu_2 compounds there is evidence that the strong single ion anisotropy [7] alone cannot explain the behavior of the magnetic excitations. The importance of anisotropy in two ions exchange interactions has been investigated in some cubic and hexagonal systems, see *e.g.* the case of TbP [8], RSb [9] and Pr [10]. In Pr and TbP the anisotropy of bilinear exchange could be demonstrated by a splitting of otherwise degenerate excitations, in CeSb this anisotropy results in a soft mode at another position than the ordering wave vector of the system. The latter, outstanding feature was found also in the present investigation on $NdCu_2$ and strongly underlines the presence of anisotropic exchange interactions. There is also another, more quantitative argument for the importance of anisotropic exchange in $NdCu_2$, which due to its length is presented in Appendix A.

After having commented the experimental evidence for anisotropic exchange, the most general bilinear exchange interaction allowed by symmetry will now be discussed.

The RCu_2 compounds crystallize in the $CeCu_2$ structure (space group *Imma*, D_{2h}^{28}), which can be thought of as an orthorhombic distortion of the hexagonal AlB_2 structure [11] (space group P_6mmm, D_{6h}^1, note that $LaCu_2$ crystallizes in this hexagonal structure). The orthorhombic *b* axis corresponds to the hexagonal axis and the *ac* plane to the hexagonal plane. Figure 4 shows the $CeCu_2$ structure in a projection into the *ac* plane, so that this correspondence can be seen clearly.

Table 1 gives the interaction tensor for the most general case of 4 equivalent neighbors (all situated in one *ab* plane) and, in addition to that, 3 more special cases. Any two ions contribution to the exchange can be classified according to the 4 cases in Table 1. *E.g.* for ions separated only in *c* direction the exchange is diagonal (this follows from the mirror symmetry of the *ac* and *bc* planes). For all other types of neighbors exchange with off diagonal elements is allowed by the orthorhombic symmetry.

In the following calculation all off-diagonal terms in the exchange will be neglected. This results in short analytical expressions for the magnetic excitation energies, but it must be kept in mind, that this approach might be too simple when comparing the calculation with the experiment.

In addition to this simplification a further restriction is used in the fitting of the exchange parameters

Table 1. General bilinear magnetic interaction tensors between Nd^{3+} ions in $NdCu_2$.

exchange tensor $\bar{\bar{\mathcal{J}}}(ij)$	distance $\mathbf{R}_i - \mathbf{R}_j$
$\begin{pmatrix} \mathcal{J}^{aa} & \mathcal{J}^{ab} & \mathcal{J}^{ac} \\ \mathcal{J}^{ba} & \mathcal{J}^{bb} & \mathcal{J}^{bc} \\ \mathcal{J}^{ca} & \mathcal{J}^{cb} & \mathcal{J}^{cc} \end{pmatrix}, \begin{pmatrix} \mathcal{J}^{aa} & -\mathcal{J}^{ab} & -\mathcal{J}^{ac} \\ -\mathcal{J}^{ba} & \mathcal{J}^{bb} & \mathcal{J}^{bc} \\ -\mathcal{J}^{ca} & \mathcal{J}^{cb} & \mathcal{J}^{cc} \end{pmatrix}$	$\begin{pmatrix} R^a \\ R^b \\ R^c \end{pmatrix}, \begin{pmatrix} -R^a \\ R^b \\ R^c \end{pmatrix}$
$\begin{pmatrix} \mathcal{J}^{aa} & \mathcal{J}^{ab} & -\mathcal{J}^{ac} \\ \mathcal{J}^{ba} & \mathcal{J}^{bb} & -\mathcal{J}^{bc} \\ -\mathcal{J}^{ca} & -\mathcal{J}^{cb} & \mathcal{J}^{cc} \end{pmatrix}, \begin{pmatrix} \mathcal{J}^{aa} & -\mathcal{J}^{ab} & \mathcal{J}^{ac} \\ -\mathcal{J}^{ba} & \mathcal{J}^{bb} & -\mathcal{J}^{bc} \\ \mathcal{J}^{ca} & -\mathcal{J}^{cb} & \mathcal{J}^{cc} \end{pmatrix}$	$\begin{pmatrix} -R^a \\ -R^b \\ R^c \end{pmatrix}, \begin{pmatrix} R^a \\ -R^b \\ R^c \end{pmatrix}$
$\begin{pmatrix} \mathcal{J}^{aa} & 0 & \mathcal{J}^{ac} \\ 0 & \mathcal{J}^{bb} & 0 \\ \mathcal{J}^{ca} & 0 & \mathcal{J}^{cc} \end{pmatrix}, \begin{pmatrix} \mathcal{J}^{aa} & 0 & -\mathcal{J}^{ac} \\ 0 & \mathcal{J}^{bb} & 0 \\ -\mathcal{J}^{ca} & 0 & \mathcal{J}^{cc} \end{pmatrix}$	$\begin{pmatrix} R^a \\ 0 \\ R^c \end{pmatrix}, \begin{pmatrix} -R^a \\ 0 \\ R^c \end{pmatrix}$
$\begin{pmatrix} \mathcal{J}^{aa} & 0 & 0 \\ 0 & \mathcal{J}^{bb} & \mathcal{J}^{bc} \\ 0 & \mathcal{J}^{cb} & \mathcal{J}^{cc} \end{pmatrix}, \begin{pmatrix} \mathcal{J}^{aa} & 0 & 0 \\ 0 & \mathcal{J}^{bb} & -\mathcal{J}^{bc} \\ 0 & -\mathcal{J}^{cb} & \mathcal{J}^{cc} \end{pmatrix}$	$\begin{pmatrix} 0 \\ R^b \\ R^c \end{pmatrix}, \begin{pmatrix} 0 \\ -R^b \\ R^c \end{pmatrix}$
$\begin{pmatrix} \mathcal{J}^{aa} & 0 & 0 \\ 0 & \mathcal{J}^{bb} & 0 \\ 0 & 0 & \mathcal{J}^{cc} \end{pmatrix}$	$\begin{pmatrix} 0 \\ 0 \\ R^c \end{pmatrix}$

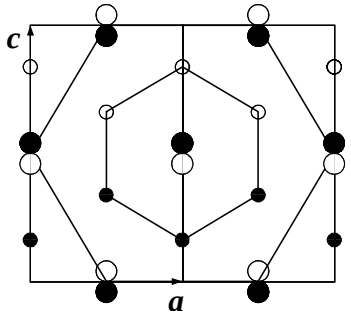

Fig. 4. Structure of $NdCu_2$ projected into the *ac* plane. The correspondence of the orthorhombic $CeCu_2$ structure to the hexagonal AlB_2 structure is indicated. The big circles indicate the Nd atoms at $y_{Nd} = 0.25$ (filled) and $y_{Nd} = 0.75$ (open), the small circles indicate the Cu atoms at $y_{Cu} = 0.0511$ and 0.4489 (filled) and $y_{Cu} = 0.5511$,0.9489 (open).

to the experimental data. It is assumed that the magnetic exchange constants "do not see" the orthorhombic distortion of the hexagonal lattice (compare Fig. 4) and in addition the exchange is isotropic for magnetic moments in the *ac* plane (*i.e.* $\mathcal{J}^{aa} = \mathcal{J}^{cc}$, $\mathcal{J}^{ac} = 0$). This assumption is asserted also by the analysis of other RCu_2 compounds, for instance $DyCu_2$. A high magnetic field along the *c* direction of $DyCu_2$ leads to a big hysteresis with a sudden increase of the saturation moment to the value of 8.5 $\mu_B/f.u.$ [12]. Afterwards the magnetic and magneto elastic behavior of the *c* axis resembles closely that of the original *a* axis (and *vice versa*). Therefore this behavior is called "conversion of the easy axis from *a* to *c*". The magnetic phase diagram after this axis conversion has been studied in detail for fields along *c* [13] and agrees in all details (within 0.5 K and 0.1 T) with that of the original *a* axis. Preliminary neutron scattering experiments in the converted state indicate, that the ordering wave vector does not change after the axis conversion [14]. This experimental evidence underlines the assumption, that in RCu_2 compounds the exchange is isotropic in the *ac* plane within a few μeV. Another case of interest in this respect is $GdCu_2$: In this compound the magnetic structure is compatible with hexagonal symmetry, it is just the lattice which shows an orthorhombic distortion. However, the lattice becomes more hexagonal at the ordering temperature, as can be seen by the change of the a/c ratio [15]. These results justify the assumption that the exchange is isotropic in the *ac* plane.

Assuming hexagonal symmetry Figure 5 shows the different types of neighbors. The numbers indicate, which of the exchange constants are related by orthorhombic symmetry only.

Bearing in mind the assumptions about the magnetic exchange the detailed calculation of the low energy magnetic excitations in the field induced ferromagnetic phase of $NdCu_2$ is performed in the mean field (MF)-random phase approximation (RPA). This method has the advantage compared to linearized spin wave theory that it is very easy to introduce the magnetic single ion anisotropy caused by the crystal field [16]. The magnetic anisotropy, both of single ion and two ions type, produces a gap in the excitation spectra.

The starting point of the calculation is the following Hamiltonian, consisting of a single ion and a two ions part:

$$H = \sum_{i,lm} B_l^m O_l^m(\mathbf{J}_i) - g_J \mu_B \sum_i \mathbf{J}_i \mathbf{B} - \frac{1}{2} \sum_{ij} \mathbf{J}_i \bar{\bar{\mathcal{J}}}(ij) \mathbf{J}_j. \tag{1}$$

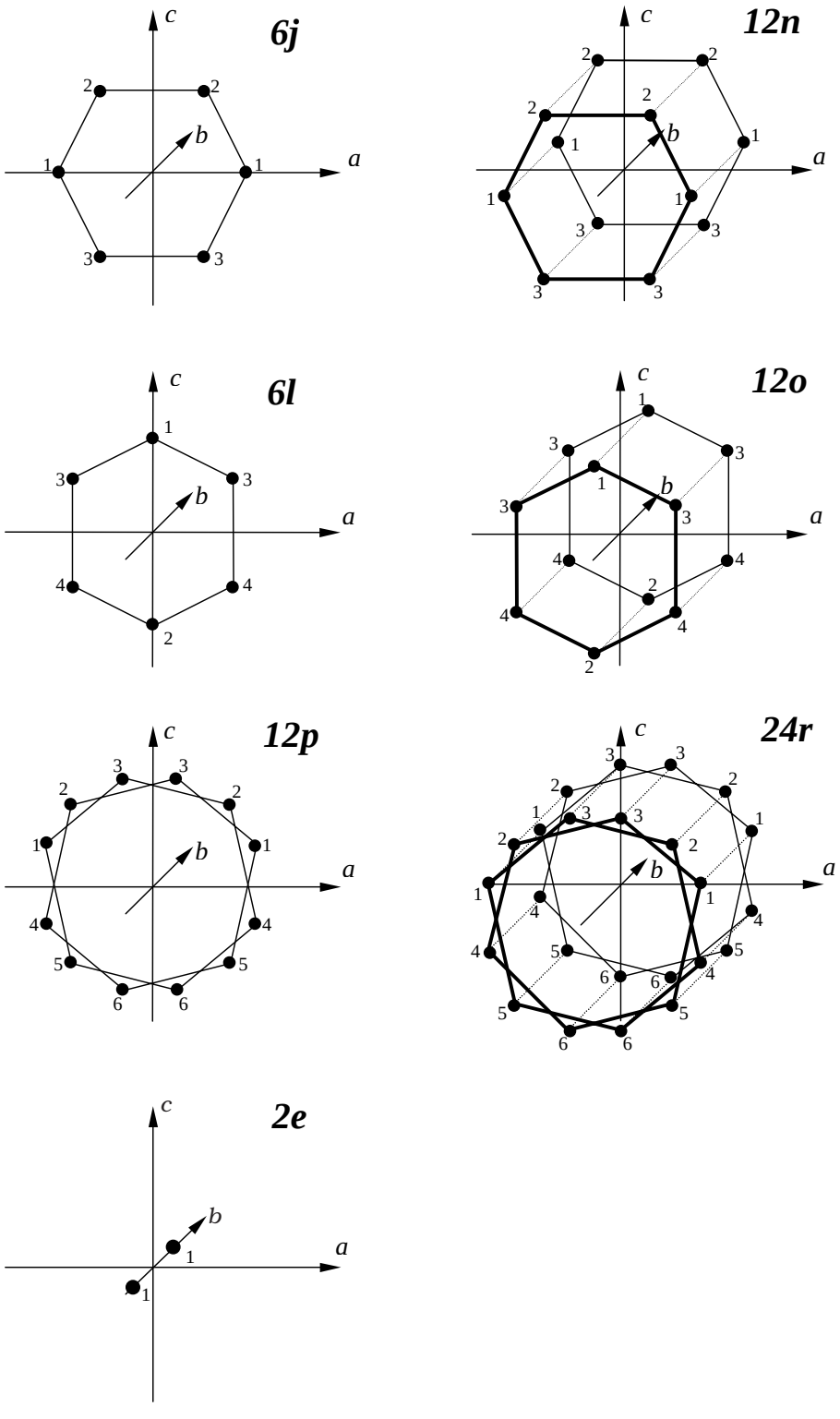

Fig. 5. Different types of bilinear exchange interactions in RCu_2 compounds assuming hexagonal symmetry of the exchange. The numbers indicate which of the exchange constants are related by orthorhombic symmetry only.

$$\overline{\overline{\mathcal{J}}}(\mathbf{Q}) = \begin{pmatrix} \overline{\overline{\mathcal{J}}}_{\mathrm{S}}(\mathbf{Q}) & \overline{\overline{\mathcal{J}}}_{\mathrm{D}}(\mathbf{Q})\exp[\mathrm{i}\mathbf{Q}(\mathbf{r}_1-\mathbf{r}_2)] \\ \overline{\overline{\mathcal{J}}}^{*}_{\mathrm{D}}(\mathbf{Q})\exp[-\mathrm{i}\mathbf{Q}(\mathbf{r}_1-\mathbf{r}_2)] & \overline{\overline{\mathcal{J}}}_{\mathrm{S}}(\mathbf{Q}) \end{pmatrix} \tag{13}$$

$$\overline{\overline{\mathcal{J}}}_{\mathrm{S}}(\mathbf{Q}) = \sum_{j}^{i,j \text{ same sublattice}} \overline{\overline{\mathcal{J}}}(ij)\exp[-\mathrm{i}\mathbf{Q}(\mathbf{R}_i-\mathbf{R}_j)] \tag{14}$$

$$\overline{\overline{\mathcal{J}}}_{\mathrm{D}}(\mathbf{Q}) = \sum_{j}^{i,j \text{ different sublattice}} \overline{\overline{\mathcal{J}}}(ij)\exp[-\mathrm{i}\mathbf{Q}(\mathbf{R}_i-\mathbf{R}_j)]. \tag{15}$$

In this expression the first term describes the crystal field [17], the second the Zeeman energy and the third the anisotropic bilinear exchange. At very low temperatures the magnetic properties may be calculated by considering only the ground state doublet $|\pm\rangle$ of the crystal field split multiplet.

In [4] the crystal field parameters have been estimated to $B_2^0 = 117\ \mu$eV, $B_2^2 = 134\ \mu$eV, $B_4^0 = 1.92\ \mu$eV, $B_4^2 = 0.87\ \mu$eV, $B_4^4 = 1.69\ \mu$eV, $B_6^0 = 0.0476\ \mu$eV, $B_6^2 = 0.0116\ \mu$eV, $B_6^4 = 0.0421\ \mu$eV and $B_6^6 = 0.366\ \mu$eV. The corresponding ground state doublet is given by $|\pm\rangle = -0.0487|\pm 9/2\rangle - 0.891|\mp 7/2\rangle + 0.373|\pm 5/2\rangle + 0.23|\mp 3/2\rangle - 0.111|\pm 1/2\rangle$. However, the following analysis does neither depend on any particular choice of crystal field parameters nor on the form of the ground state.

The Hamiltonian (1) may be projected into the ground state doublet yielding (for external fields B parallel to the b axis, the coordinates are chosen such that $a\|x, c\|y, b\|z$)

$$\begin{aligned} H = E_0 &- g_{\mathrm{J}}\mu_{\mathrm{B}}\sum_i \begin{pmatrix} M & 0 \\ 0 & -M \end{pmatrix}_i B \\ &- \frac{1}{2}\sum_{ij} \begin{pmatrix} 0 & A \\ A & 0 \end{pmatrix}_i \mathcal{J}^{aa}(ij) \begin{pmatrix} 0 & A \\ A & 0 \end{pmatrix}_j \\ &- \frac{1}{2}\sum_{ij} \begin{pmatrix} M & 0 \\ 0 & -M \end{pmatrix}_i \mathcal{J}^{bb}(ij) \begin{pmatrix} M & 0 \\ 0 & -M \end{pmatrix}_j \\ &- \frac{1}{2}\sum_{ij} \begin{pmatrix} 0 & C \\ -C & 0 \end{pmatrix}_i \mathcal{J}^{cc}(ij) \begin{pmatrix} 0 & C \\ -C & 0 \end{pmatrix}_j \end{aligned} \tag{2}$$

$$A = \langle +|J^a|-\rangle \qquad A^* = A \tag{3}$$

$$\pm M = \langle \pm|J^b|\pm\rangle \qquad M^* = M \tag{4}$$

$$C = \langle +|J^c|-\rangle \qquad C^* = -C. \tag{5}$$

A mean field (MF) is introduced and the splitting of the ground state $\Delta = E_- - E_+$ is calculated selfconsistently according to the following relations (taking into account interdoublet mixing to second order in B^{eff} as described in [3] Eqs. (8, 9)).

$$B^{\mathrm{eff}} = B + \frac{1}{g_{\mathrm{J}}\mu_{\mathrm{B}}}\mathcal{J}^{bb}(\mathbf{q}=0)\langle J^b\rangle \tag{6}$$

with the thermal expectation value defined as

$$\langle J^b\rangle = M^+ n_+ + M^- n_- \tag{7}$$

$$M^{\pm} = \pm M(1 \pm \alpha B^{\mathrm{eff}}) \tag{8}$$

$$E_\pm - E_0 = \mp g_{\mathrm{J}}\mu_{\mathrm{B}} M(1 \pm \alpha B^{\mathrm{eff}}/2)B^{\mathrm{eff}} \tag{9}$$

$$n_\pm = \frac{\exp(-E_\pm/k_{\mathrm{B}}T)}{\exp(-E_+/k_{\mathrm{B}}T) + \exp(-E_-/k_{\mathrm{B}}T)}\,. \tag{10}$$

In this expression $n_\pm$ are the thermal population numbers of the two states $|\pm\rangle$ split by the effective field B^{eff}. The Fourier transform of the exchange tensor $\overline{\overline{\mathcal{J}}}(ij)$ (*i.e.* $\mathcal{J}^{bb}(\mathbf{q}=0)$) is defined in equation (A.3).

The frequency dependent single ion susceptibility $\overline{\overline{\chi_0}}\ (\omega)$ can be calculated for the MF ground state doublet

$$\overline{\overline{\chi_0}}\ (\omega) = \begin{pmatrix} \frac{nA^2\Delta}{\Delta^2-\hbar^2\omega^2} & 0 & \frac{nAC\hbar\omega}{\Delta^2-\hbar^2\omega^2} \\ 0 & \chi_0^{bb} & 0 \\ -\frac{nAC\hbar\omega}{\Delta^2-\hbar^2\omega^2} & 0 & -\frac{nC^2\Delta}{\Delta^2-\hbar^2\omega^2} \end{pmatrix} \tag{11}$$

with the abbreviation $n = 2(n_- - n_+) \overset{T\to 0}{\longrightarrow} 2$. χ_0^{bb} is zero for $\omega \neq 0$ and will therefore be neglected in the following calculation.

A first estimate for the order of the excitation energies are the singularities of this single ion susceptibility (*i.e.* at $\hbar\omega = \Delta$). To describe the dispersion correctly the two-atomic basis in this compound is taken into account and RPA is performed (compare [16]) to calculate the susceptibility $\overline{\overline{\chi}}\ (\mathbf{Q},\omega)$

$$\overline{\overline{\chi}}\ (\mathbf{Q},\omega) = \left[\begin{pmatrix} \overline{\overline{\chi_0}}\ (\omega) & 0 \\ 0 & \overline{\overline{\chi_0}}\ (\omega) \end{pmatrix}^{-1} - \overline{\overline{\mathcal{J}}}(\mathbf{Q}) \right]^{-1}. \tag{12}$$

This is an equation of 6×6 matrices (for each of the Nd atoms in the basis of the crystal there is a single ion excitation matrix). The Fourier transform of the coupling is given by

see equations (13, 14, 15) above.

In this expression the $\mathbf{R}_i$ are the position vectors of the Nd^{3+} ions, $(\mathbf{r}_1 - \mathbf{r}_2)$ designates the position of one Nd sublattice with respect to the other Nd sublattice. According to the fluctuation dissipation theorem (see [16])

the neutron cross-section is then given by summing over the components of $\overline{\overline{\chi}}''(\mathbf{Q},\omega) = (\overline{\overline{\chi}}(\mathbf{Q},\omega) - \overline{\overline{\chi}}^{\dagger}(\mathbf{Q},\omega))/2\mathrm{i}$

$$\frac{\mathrm{d}\sigma}{\mathrm{d}E'\mathrm{d}\Omega} = \frac{K}{1-\exp(-\hbar\omega/k_\mathrm{B}T)} \sum_{\substack{\alpha\beta\ldots \text{ spatial indices} \\ ss'\ldots \text{ sublattice indices}}} \times \chi''_{\substack{\alpha\beta \\ ss'}}(\mathbf{Q},\omega)\exp[-\mathrm{i}\mathbf{Q}(\mathbf{r}_s - \mathbf{r}_{s'})](\delta_{\alpha\beta} - \hat{Q}_\alpha\hat{Q}_\beta)$$

$$K = \frac{k_\mathrm{f}}{k_\mathrm{i}} N \frac{1}{\pi}\left(\frac{\hbar\gamma e^2}{mc^2}\right)^2 \left\{\frac{1}{2} g_\mathrm{J} F(Q)\right\}^2. \qquad (16)$$

In this expression k_i and k_f denote the wave vector of the incoming and of the scattered neutron, respectively, $F(Q)$ is the magnetic form factor of Nd^{3+} in the dipole approximation, N the number of scattering Nd atoms, $\gamma = g_\mathrm{n}/2\hbar$ the gyromagnetic ratio of the neutron and $e^2/mc^2 = 2.82$ fm is the classical electron radius.

The excitation energies can be calculated by analyzing the poles of this cross-section. If the exchange is assumed to be isotropic in the ac plane, $\overline{\overline{\mathcal{J}}}_\mathrm{S}(\mathbf{Q})$ and $\overline{\overline{\mathcal{J}}}_\mathrm{D}(\mathbf{Q})$ are diagonal and the aa and cc components are equal. Using the notation $\mathcal{J}_\mathrm{D}(\mathbf{Q}) = \mathcal{J}_\mathrm{D}^{aa}(\mathbf{Q}) = \mathcal{J}_\mathrm{D}^{cc}(\mathbf{Q})$, $\mathcal{J}_\mathrm{S}(\mathbf{Q}) = \mathcal{J}_\mathrm{S}^{aa}(\mathbf{Q}) = \mathcal{J}_\mathrm{S}^{cc}(\mathbf{Q})$ (but still assuming that $\mathcal{J}_\mathrm{S}^{aa}(\mathbf{Q}) \neq \mathcal{J}_\mathrm{S}^{bb}(\mathbf{Q})$ and $\mathcal{J}_\mathrm{D}^{aa}(\mathbf{Q}) \neq \mathcal{J}_\mathrm{D}^{bb}(\mathbf{Q})$) it is possible to derive an analytical expression for the cross-section of the magnetic excitations by combining equations (11–16):

$$\frac{\mathrm{d}\sigma}{\mathrm{d}E'\mathrm{d}\Omega} = \frac{2Kn}{1-\exp(-\hbar\omega/k_\mathrm{B}T)} \Im\left(\frac{f\hbar^2\omega^2 + g}{\hbar^4(\omega_1^2-\omega^2)(\omega_2^2-\omega^2)}\right)$$

$$f = (1-\hat{Q}_a^2)A^2(\Re(v) - s) - C^2(1-\hat{Q}_c^2)(\Re(u) - r)$$

$$g = (1-\hat{Q}_a^2)A^2(s^2 - v^\star v)[r + \Re(u)] - (1-\hat{Q}_c^2)C^2(r^2 - u^\star u)[s + \Re(v)]$$

$$r = \Delta - nA^2\mathcal{J}_\mathrm{S}(\mathbf{Q})$$

$$s = \Delta + nC^2\mathcal{J}_\mathrm{S}(\mathbf{Q})$$

$$u = nA^2\mathcal{J}_\mathrm{D}(\mathbf{Q})$$

$$v = -nC^2\mathcal{J}_\mathrm{D}(\mathbf{Q}). \qquad (17)$$

In this expression $\Re$ and $\Im$ denote real and imaginary parts. The excitation energies $\hbar\omega_1$ and $\hbar\omega_2$ are given by

$$[\hbar\omega_{\frac{1}{2}}]^2 = \{\Delta - nA^2[\mathcal{J}_\mathrm{S}(\mathbf{Q}) \mp |\mathcal{J}_\mathrm{D}(\mathbf{Q})|]\} \times \{\Delta + nC^2[\mathcal{J}_\mathrm{S}(\mathbf{Q}) \mp |\mathcal{J}_\mathrm{D}(\mathbf{Q})|]\}. \qquad (18)$$

The corresponding intensities I_1 and I_2 can be calculated from the residua of equation (17) – note that any factors arising from the scattering geometry of a triple axis spectrometer are not included in the following expression:

$$I_{\frac{1}{2}} = \frac{Kn}{2\hbar\omega_{\frac{1}{2}}(1-\exp(-\hbar\omega_{\frac{1}{2}}/k_\mathrm{B}T))}\left(1 \mp \frac{\Re[\mathcal{J}_\mathrm{D}(\mathbf{Q})]}{|\mathcal{J}_\mathrm{D}(\mathbf{Q})|}\right) \times \{(1-\hat{Q}_a^2)A^2(s \pm |v|) - (1-\hat{Q}_c^2)C^2(r \pm |u|)\}. \qquad (19)$$

Note that $\mathcal{J}_\mathrm{S}(\mathbf{Q})$ and $\mathcal{J}_\mathrm{D}(\mathbf{Q})$ transform under a translation about $(1\ \ 1\ \ 0)$ as $\mathcal{J}_\mathrm{S}(\mathbf{Q} + (1\,1\,0)) = \mathcal{J}_\mathrm{S}(\mathbf{Q})$ and $\mathcal{J}_\mathrm{D}(\mathbf{Q} + (1\,1\,0)) = -\mathcal{J}_\mathrm{D}(\mathbf{Q})$. Inserting this property into equations (18, 19) one finds, that $\hbar\omega_1(\mathbf{Q} + (1\,1\,0)) = \hbar\omega_1(\mathbf{Q})$ and $\hbar\omega_2(\mathbf{Q} + (1\,1\,0)) = \hbar\omega_2(\mathbf{Q})$. Neglecting the $\mathbf{Q}$ dependence of K for the moment (which is small due to the magnetic form factor), we see, that the intensities of the two excitations are exchanged by this translation, *i.e.* $I_1(\mathbf{Q} + (1\,1\,0)) = I_2(\mathbf{Q})$ and $I_2(\mathbf{Q} + (1\,1\,0)) = I_1(\mathbf{Q})$.

If neutron experiments are performed in the reciprocal ab plane, $\mathcal{J}_\mathrm{D}(\mathbf{Q})$ is real and according to equation (19) either $I_1(\mathbf{Q})$ or $I_2(\mathbf{Q})$ is zero. Only one excitation can be observed for a given wave vector $\mathbf{Q}$, the other branch can be measured at $\mathbf{Q} + (1\,1\,0)$.

However, such favorable experimental conditions can be used only to measure the dispersion for $l = 0$. For $l \neq 0$ the calculation always predicts two excitations.

5 Numerical analysis of the magnetic excitations in $NdCu_2$

For the transition matrix elements A and C defined in equation (3) the values $A = 2.00$ and $C = i1.6$ have been used. This is in reasonable agreement with the values deduced from magnetization at 8 K [7] (*i.e.* $A = 2.1$, $C = i1.5$) and those derived from the published crystal field parameters [4] (*i.e.* $A = 2.0$, $C = i1.5$). Scaling of both of these parameters scales the amplitude of the dispersion. Changing the relation of the values of A to C affects the form of the dispersion: the steepness of the low energy modes is increased while the high energy modes become flatter if A and C become very different (see Eq. (18)).

For the determination of Δ and B^eff the following parameters have been used in equations (2–10): $M = 2.27$, $\alpha = 0.03\ \mathrm{T}^{-1}$ and $\mathcal{J}^{bb}(\mathbf{q} = 0) = 24.6\ \mu\mathrm{eV}$ (*i.e.* the same as in [3]). Solving equations (2–10) selfconsistently with respect to Δ and B^eff for $B = 3T$ gives $\Delta = 0.861$ meV and $B^\mathrm{eff} = 4.50$ T.

Using the above value for Δ, only an insufficient fit of the observed dispersion could be achieved. To improve the fit, Δ was varied (yielding $\Delta = 1.106$ meV) and the standard deviation (described below by Eq. (20)) could be reduced to 20% of its former value. This indicates, that the value of Δ derived from the study of the magnetic phase diagram [3] at 3 T external field is too low, suggesting that $\mathcal{J}^{bb}(q = 0)$ has to be modified. A consistent description can be obtained with $\mathcal{J}^{bb}(q = 0) = 44\ \mu$eV, $B^\mathrm{eff} = 5.78$ T and $\Delta = 1.106$ meV. The new value for $\mathcal{J}^{bb}(q = 0)$ can be used as an input for refining the calculation of the exchange parameters $\mathcal{J}^{bb}(ij)$ describing the magnetic phase diagram (compare [3]).

The exchange parameters $\mathcal{J}^{aa}(ij) = \mathcal{J}^{cc}(ij)$ have been obtained by performing a least square fit of the calculated to the measured dispersion using a simulated annealing algorithm [18]. The following expression was minimized ($E_1(\mathbf{Q})$ and $E_2(\mathbf{Q})$ denote the measured modes, $s_1(\mathbf{Q})$ and $s_2(\mathbf{Q})$ some statistical weighting factors and

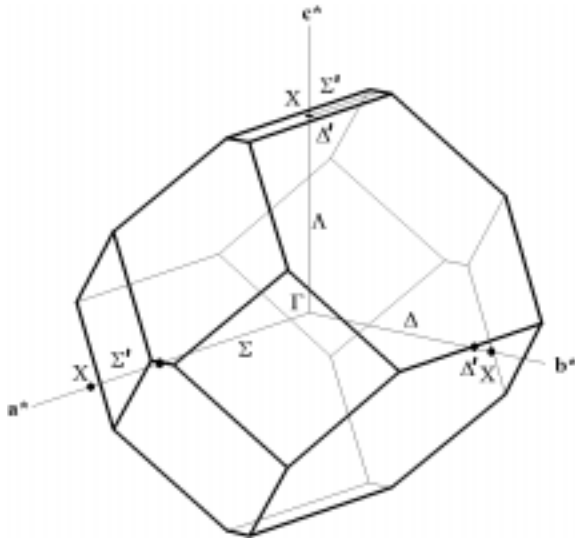

Fig. 6. First Brillouin zone of $NdCu_2$, the Γ–point, the X–point and the main symmetry directions are indicated.

$\Theta(x)$ the step function):

$$\sum_{\mathbf{Q}\in\{\text{measured constant Q-scans}\}} s_1(\mathbf{Q})[\hbar\omega_1(\mathbf{Q}) - E_1(\mathbf{Q})]^2 + s_2(\mathbf{Q})[\hbar\omega_2(\mathbf{Q}) - E_2(\mathbf{Q})]^2 + \sum_{i=1,2,\mathbf{Q}\in\{\text{1st Brillouin zone}\}\atop |\mathbf{Q}-(0.65\,1\,0)|>0.15\ \text{Å}^{-1}} \Theta(0.73\ \text{meV} - \hbar\omega_i(\mathbf{Q})) \times \frac{1+\Theta(0.63\ \text{meV} - \hbar\omega_i(\mathbf{Q}))}{2}[\hbar\omega_i(\mathbf{Q}) - 0.73\ \text{meV}]^2. \quad (20)$$

The second sum in equation (20) ensures, that the minimum of the dispersion relation at $\mathbf{q} = (0.65\,1\,0)$ is a global minimum. In this sum only $\mathbf{q}$ vectors in the first Brillouin zone with positive h, k and l have been considered, because the excitation energies in the other parts of the zone are related by symmetry (compare Eq. (18)). The error in the fitted exchange parameters was estimated from the experimental error in the measurement. Assuming an average experimental error of 0.15 meV leads to a variation of (20) by about 0.14 meV^2. This variation corresponds to a variation of the fitting parameters within the range of the error bars shown in Figure 8. Note that an error estimation obtained in this way does not take into account the fact, that there might be several isolated solutions in other regions of the parameter space. Figure 6 shows the first Brillouin zone and the main symmetry directions of the reciprocal lattice. The primed letters denote the extension of a symmetry line from the zone boundary to the X–point. Note that for the related hexagonal lattice the Brillouin zone would have the shape of a simple honeycomb with $\Sigma'/\Sigma = 1/2$.

Using a set of fitted parameters and formula (18) the excitation energies have been calculated. Figure 7 shows, how the calculated excitation energies compare to the experimental data. The dispersion along Λ shows a fast oscillation with $\mathbf{q}$ indicating the long range of the exchange. It was necessary to include the neighbor $\mathbf{r} = (0, 0, 2c)$ (distance: 15 Å) into the model to explain this oscillating behavior (or alternatively assume non hexagonal exchange resulting in a model with even more parameters and different signs of parameters which in hexagonal description should be equal). This high frequency in Fourier space was also observed in the magnetic excitations of $PrCu_2$ [19]. In Σ direction the position of the minimum in the dispersion and the mode crossing are in excellent agreement with the available experimental data. Also the two weakly dispersive modes along Δ compare well to the calculation.

In addition to the peak positions which are shown in Figure 7, the intensities have been evaluated and compared to the calculation (19). The contribution of the polarization factors $(1 - \hat{Q}_a^2)$ and $(1 - \hat{Q}_c^2)$ dominates and results in strong intensities for $\mathbf{Q} \parallel b$. The relative intensity of the two modes is correctly described by the model. For instance along the $(h\ \ 0\ \ 1)$ direction the intensity of the dispersive mode is only 10 percent of the intensity of the other mode. Along $(h\ \ 0\ \ 2)$ both modes have about the same intensity (difference less than 30 percent – compare the experimental data in Fig. 2). A calculation assuming hexagonal symmetry of the structure gives only one excitation. Comparing such a calculation to the experiment showed, that whenever two excitations are observed, the weaker excitation (*i.e.* the upper mode along $(0\ \ 0\ \ l)$ and the strongly dispersive mode along $(h\ \ 0\ \ 1)$ and $(h\ \ 0\ \ 2)$) is expected to disappear in hexagonal symmetry.

More accurate experimental data would be needed for a comparison of small details in the variation of the intensity, which are due to the oscillations in $\mathcal{J}_S(\mathbf{Q})$ and $\mathcal{J}_D(\mathbf{Q})$.

Figure 8 shows the dependence of the fitted exchange constants $\mathcal{J}^{aa} = \mathcal{J}^{cc}$ on the interatomic distance. The different types of neighbors are indicated by different symbols. Because of the orthorhombic distortion of the lattice the distance varies within some sets of exchange constants, which have been kept equal in the fit process because of the nearly hexagonal symmetry. The exchange constants of type $2e$, indicated by the filled triangles in Figure 8 appear rather large. If these constants are set to a smaller value, the quality of the fit deteriorates dramatically. The large contribution might be connected with the fact, that the parameters of type $2e$ describe the exchange between Nd^{3+} ions situated in a zig zag chain in b direction with very short distance, whereas for all other types of interactions one or more Cu atoms are situated in or near the connecting line. The dashed line in Figure 8 represents the magnitude of the classical dipole – dipole interaction, the solid line

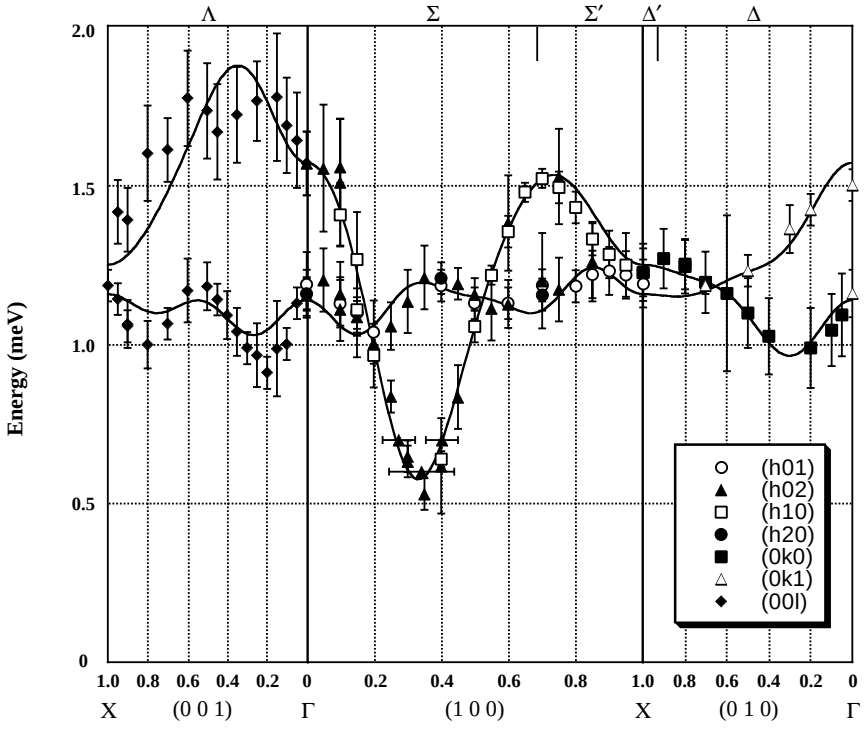

Fig. 7. **Q**-dependence of the magnetic excitations in the field induced ferromagnetic phase of $NdCu_2$ at $\mu_0 H \parallel b = 3$ T, the lines show the dispersion as calculated by the MF-RPA model described in the text.

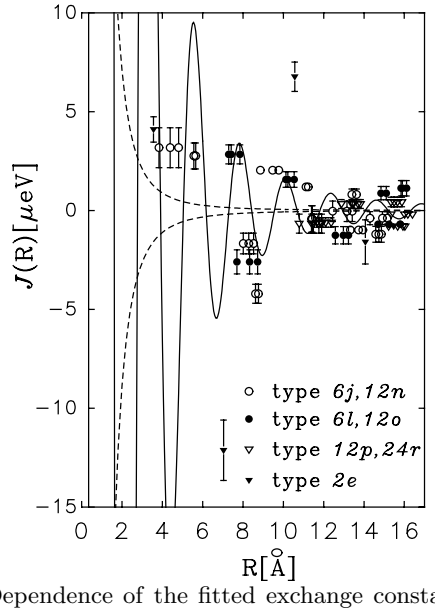

Fig. 8. Dependence of the fitted exchange constants on the interatomic distance. The different types of neighbors are indicated by different symbols. The full lines show the indirect exchange interaction as given by a free electron model described in the text. The dashed lines show the magnitude of the classical dipolar exchange (*i.e.* $+2(g_J\mu_B)^2/R^3$ and $-5(g_J\mu_B)^2/2R^3$).

shows the indirect exchange interaction as given by a free electron model [16]. The corresponding formulas are

$$\mathcal{J}^{\alpha\beta}(ij) = (g_J\mu_B)^2 \frac{3(R_i^\alpha - R_j^\alpha)(R_i^\beta - R_j^\beta) - |\mathbf{R}_i - \mathbf{R}_j|^2}{|\mathbf{R}_i - \mathbf{R}_j|^5} \tag{21}$$

for the classical dipole exchange and

$$\mathcal{J}^{\alpha\beta}(ij) = \delta_{\alpha\beta} 12\pi\nu |j_0|^2 \bar{\mathcal{N}}(\tilde{\epsilon}_F) \times \frac{\sin(2k_F|\mathbf{R}_i - \mathbf{R}_j|) - 2k_F|\mathbf{R}_i - \mathbf{R}_j|\cos(2k_F|\mathbf{R}_i - \mathbf{R}_j|)}{2k_F|\mathbf{R}_i - \mathbf{R}_j|^4} \tag{22}$$

for the indirect exchange interaction in a simple isotropic model (RKKY) [16]. In the above expression ν denotes the number of conduction electrons/f.u. (*i.e.* $\nu = 5 = 3[\mathrm{Nd}] + 2 \times 1[\mathrm{Cu}]$), j_0 the effective *s-f* exchange integral (*i.e.* $j_0 \sim (g_J - 1)0.1$ eV), $k_F = 1.395$ Å^{-1} the Fermi wave vector in a free electron model [20] and $\bar{\mathcal{N}}(\tilde{\epsilon}_F)$ the density of electronic states/f.u. (*i.e.* ~ 2.8 eV^{-1}; this value corresponds to the specific heat γ–value in YCu_2 of 6.7 mJ/mol K^2). To compare with the experimentally determined exchange constants the indirect exchange (RKKY) had to be scaled by a factor 0.06.

The classical dipolar exchange is comparable to the indirect RKKY exchange only for neighbors up to 6 Å, especially for next neighbors in the quasi – hexagonal *ac* plane. It is obviously non diagonal (this fact is neglected in the present analysis of the magnetic excitations) and therefore might drive the formation of the noncollinear magnetic structure observed in $GdCu_2$ [15].

Figure 9 shows the Fourier transform of the exchange interaction constants $\mathcal{J}^{bb}(\mathbf{Q})$ (as determined by the magnetic phase diagram [3], compare equation (A.3)) and $\mathcal{J}^{aa}(\mathbf{Q}) = \mathcal{J}^{cc}(\mathbf{Q}) = \mathcal{J}_S(\mathbf{Q}) + \mathcal{J}_D(\mathbf{Q})$ (as determined by the magnetic excitations in the field induced ferromagnetic phase F3). The difference of the dashed and full line

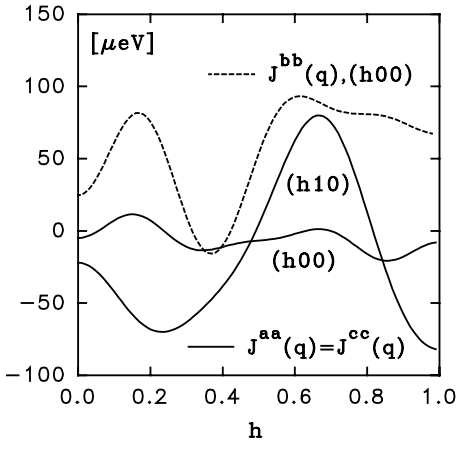

Fig. 9. Fourier transform of the fitted exchange interaction of $NdCu_2$ for moments in the quasi – hexagonal plane ($\mathcal{J}^{aa}(\mathbf{Q}) = \mathcal{J}^{cc}(\mathbf{Q})$) and for moments in b direction ($\mathcal{J}^{bb}(\mathbf{Q})$). Note that the curve of $\mathcal{J}^{bb}(\mathbf{Q})$ has been taken from the parameters used to describe the phase diagram in [3] and should be modified at $Q = 0$ according to the present analysis discussed in the text.

in (h 0 0) direction is a measure of the anisotropy of the exchange. The wavelength of the oscillations with $\mathbf{q}$ is inversely related to the range of the exchange interactions, indicating the importance of distant neighbor interactions in $NdCu_2$.

6 Magnetic order in other RCu_2 compounds

Having analyzed the exchange in such detail for $NdCu_2$ one question is obvious: Is it possible to interpret the ordering process of other RCu_2 compounds (R = Ce, Pr, Sm, Gd, Tb, Dy, Ho, Er, Tm) on the basis of these parameters?

The exchange parameters given in Figure 8 can be used to make a prediction for the ordering temperature and the magnetic structure of some other RCu_2 compounds on the basis of a MF theory. For simplicity we assume, that the CF anisotropy of the rare earth moments can be described by considering an anisotropic two level system (except in the case of Gd, where CF effects can be neglected). The anisotropy of this two level system is estimated by the saturation value of the magnetic moment components $\mu^{\rm sat}_{a,b,c} = g_{\rm J}\mu_{\rm B}M_{a,b,c}$ in the three orthorhombic axes (the corresponding matrix elements of $\mathbf{J}$, *i.e.* $M_{a,b,c}$ have been calculated from the available experimental data and are listed in the third column of Table 2 for some RCu_2 compounds).

To calculate the ordering temperatures for different possible magnetic structures the two ions exchange interactions of the present analysis of $NdCu_2$ are used. Assuming an indirect exchange interaction, $\overline{\overline{\mathcal{J}}}_{\rm Spin}(\mathbf{q})$ should be comparable among the different rare earths [16]. $\overline{\overline{\mathcal{J}}}_{\rm Spin}(\mathbf{q})$ is defined by

$$\overline{\overline{\mathcal{J}}}(\mathbf{q}) \equiv (g_{\rm J}-1)^2\,\overline{\overline{\mathcal{J}}}_{\rm Spin}(\mathbf{q}). \qquad (23)$$

Next we calculate the maximum of the Fourier transform of the exchange interaction $\mathcal{J}^{bb}(\mathbf{Q})$ and $\mathcal{J}^{aa}(\mathbf{Q}) = \mathcal{J}^{cc}(\mathbf{Q})$.

For $\mathcal{J}^{aa}(\mathbf{Q}) = \mathcal{J}^{cc}(\mathbf{Q})$ the maximum of the exchange corresponds to the minimum of the dispersion in $NdCu_2$ at $\mathbf{Q} \sim (2/3\,1\,0)$. From the present analysis of the magnetic excitations we find $\mathcal{J}^{aa}(\mathbf{Q} = (2/3\,1\,0)) = 79$ μeV (using the parameters shown in Fig. 8). This value is scaled according to equation (23) for other RCu_2 compounds and listed in column 4 of Table 2. The maximum of $\mathcal{J}^{bb}(\mathbf{Q})$ will be at about $\mathbf{Q} \sim (2/3\,0\,0)$, corresponding to the type of magnetic order found in $NdCu_2$. From the Néel temperature $T_{\rm N} = 6.5$ K we estimate $\mathcal{J}^{bb}(\mathbf{Q} = (2/3\,0\,0)) = 93$ μeV (see Fig. 9, [3]). Also this value is scaled according to equation (23) and listed in column 4 of Table 2 for other RCu_2 compounds.

With this input it is now possible to calculate ordering temperatures for moments in a or c direction

$$k_{\rm B}T^a_{\rm N} = M_a^2\mathcal{J}^{aa}(\mathbf{Q} = (2/3\,1\,0)) \qquad (24)$$

$$k_{\rm B}T^c_{\rm N} = M_c^2\mathcal{J}^{cc}(\mathbf{Q} = (2/3\,1\,0)) \qquad (25)$$

and for moments in b direction

$$k_{\rm B}T^b_{\rm N} = M_b^2\mathcal{J}^{bb}(\mathbf{Q} = (2/3\,0\,0)). \qquad (26)$$

Note that the ordering wave vector $\mathbf{Q}$ is different for magnetic moments within the ac plane and parallel to the b direction due to the different position of the maximum in $\mathcal{J}^{aa}(\mathbf{Q}) = \mathcal{J}^{cc}(\mathbf{Q})$ and $\mathcal{J}^{bb}(\mathbf{Q})$, respectively. Equations (24–26) are valid also for negligible CF anisotropy (*i.e.* $M_a \sim M_b \sim M_c$) and can be used to calculate the ordering temperatures $T^\alpha_{\rm N}$ for the two types of modulation. Naturally, only the largest value for the ordering temperature will be of physical relevance (compare [16]).

In Table 2 the calculated ordering temperatures for the different moment directions and ordering wave vectors are compared to experimental data. The calculation of the ordering temperature was performed according to equations (24–26), except for the case of Gd, where the CF splitting is negligible. For Gd the well-known formula $3k_{\rm B}T^\alpha_{\rm N} = J(J+1)\mathcal{J}^{\alpha\alpha}(\mathbf{Q})$ was used.

Of course, from such simple modeling a complete explanation of all details cannot be expected. However, in most cases the calculation is in reasonable agreement with available experimental data.

Whenever $T^a_{\rm N}$ or $T^c_{\rm N}$ show the largest value, the predicted magnetic modulation vector $\mathbf{Q}$ is equal to (2/3 1 0) (*e.g.* for $TbCu_2$ and $DyCu_2$ – see Tab. 2). For the compounds where $T^b_{\rm N}$ has been calculated to be larger than $T^a_{\rm N}$ and $T^c_{\rm N}$, $\mathbf{Q} \sim (2/3\,0\,0)$ is the predicted modulation vector. In most cases this is true.

It is of interest to compare the exchange parameters used in this paper to those obtained by Iwata *et al.* [21] for $TbCu_2$ and $DyCu_2$: In Table 3 the reduced exchange parameters of $TbCu_2$ and $DyCu_2$, which have been defined in [21], are compared to those calculated from our set for $NdCu_2$ (shown in Fig. 8).

Table 2. Calculated and experimentally observed ordering temperatures and wave vectors for some RCu_2 compounds. The saturation moment is estimated from magnetization experiments. It is used to calculate the ordering temperature for different possible magnetic structures (*i.e.* (2/3 1 0) with a or c as the easy axis, (2/3 0 0) with b as the easy axis). If the observed structure does not agree with the calculated one it is marked by a "≠".

	J	g_J	$M_a = A$ $M_b = M$ $M_c = C/i$	$\mathcal{J}^{aa}(2/3\,1\,0)$ $\mathcal{J}^{bb}(2/3\,0\,0)$ $\mathcal{J}^{cc}(2/3\,1\,0)$ [μeV]	T_N^a T_N^b T_N^c [K]	T_N^{exp}[K]	$\boldsymbol{\tau}^{exp}$
$CeCu_2$	$\frac{5}{2}$	$\frac{6}{7}$	1.9 0.6 [30] 1.3	21.7 25.5 21.7	**0.9** ≠ 0.1 0.4	3.5 [31]	$(1\,1\,0)$[2]
$PrCu_2$	4	$\frac{4}{5}$	1.9 0.9 [32] 0.4	42.5 50.0 42.5	**1.8** 0.5 0.08	[33][3]	-
$NdCu_2$	$\frac{9}{2}$	$\frac{8}{11}$	2.0 2.5 [7] 1.6	79 93 79	3.7 **6.7** 2.3	6.5 [2]	(0.618 0 0)
$SmCu_2$	$\frac{5}{2}$	$\frac{2}{7}$	0.1 0.3 [34] ?	542 638 542	0.06 **0.67** ?	23 [6]	?
$GdCu_2$	$\frac{7}{2}$	2	-	1062 1250 1062	65 **76** ≠ 65	40 [15]	(2/3 1 0) [15]
$TbCu_2$	6	$\frac{3}{2}$	5.9 0.4 [32] 1.3	266 313 266	**107** 0.6 5.2	54 [25]	(2/3 1 0) [24]
$DyCu_2$	$\frac{15}{2}$	$\frac{4}{3}$	7.4 3.8 [32] 1.9	118 139 118	**75** 23 4.9	27 [13]	(2/3 1 0) [26]
$HoCu_2$	8	$\frac{5}{4}$	6.4 4.6 [32] 2.7	66.4 78.1 66.4	**31.5** 19.2 5.6	10 [25]	(2/3 1 0) [27][4]
$ErCu_2$	$\frac{15}{2}$	$\frac{6}{5}$	0.4 7.1 [32] 0.9	42.5 50.0 42.5	0.08 **29.2** 0.40	12 [25]	(0.615 0 0) [28][5]
$TmCu_2$	6	$\frac{7}{6}$	0.7 5.9 [29] 0.9	29.5 34.7 29.5	0.2 **14.0** 0.3	6 [25]	(5/8 0 0) [29][6]

[2] Note that in $CeCu_2$ the chemical and the magnetic unit cell is identical except for the fact that the magnetic moments of the Ce ions on the two positions are coupled antiferromagnetically. This may either be described by a propagation vector (0 0 0) and a 180° phase shift or by a propagation vector (1 1 0).
[3] *i.e.* in $PrCu_2$ the magnetic order is screened by quadrupolar order at 7.5 K.
[4] for $HoCu_2$ a propagation of (1/3 0 0) has been reported [27] for the high temperature phase between 7.4 and 10 K, this is equivalent to an indexing with a propagation vector (2/3 1 0), the moments are aligned in a direction.
[5] in $ErCu_2$ a propagation of (0.385 0 0) was discussed in [28], however satellites have also been found at (0.385 0 1) = (1 0 1)–(0.615 0 0).
[6] the data of $TmCu_2$ presented in [29] can be indexed according to (5/8 0 0).

In [21] the parameters of $TbCu_2$ and $DyCu_2$ have been adjusted to reproduce the correct Néel temperature within a mean field theory (compare Eq. (24); however, in [21] the effect of all crystal field states has been considered). The magnitude of the Néel temperature T_N is determined by a linear combination of these parameters, which is compared at the bottom of Table 3. The value derived from the present analysis of $NdCu_2$ exceeds only slightly the values for the other compounds.

Using the model described by [21] and the parameters derived from the present analysis of $NdCu_2$ (third column in Tab. 3), the critical field for the spin flip to the ferromagnetic phase has been calculated for $DyCu_2$ to 6.1 T. It exceeds the experimental value of 2.0 T [13,21].

7 Conclusion

The dispersion of the magnetic excitations in the field induced ferromagnetic phase F3 of $NdCu_2$ can be described by a MF-RPA model with anisotropic magnetic bilinear R-R exchange interactions. An attempt to analyze

Table 3. Comparison of the exchange constants determined from the phase diagrams of $TbCu_2$ and $DyCu_2$ in [21] with the model presented here for $NdCu_2$.

	$TbCu_2$ [21]	$DyCu_2$ [21]	$NdCu_2$
J_1 [K]	2.65	2.09	2.47
J_2 [K]	−1.00	−1.26	−2.79
J_3 [K]	3.16	2.78	3.49
J_4 [K]	−1.69	−1.67	−3.61
$J_1 - J_2 + J_3 - J_4$[K] $(\propto T_N/(g_J-1)^2)$	8.5	7.8	12.36
$J_0 = 2J_1 + 2J_2 + J_3 + J_4$[K] $(\propto \mathcal{J}_{\rm Spin}(q=0))$	4.77	2.77	−0.77

the magnetic ordering process in other RCu_2 compounds on the basis of this model shows:

1. The direction, into which the ordered magnetic moments point, is mainly determined by the crystal field, because the CF interaction is much bigger than the R-R exchange interaction.
2. The exchange interaction between neighbors in b direction dominates, probably because the interatomic distance between these R atoms is small and therefore the magnetic interaction is not screened by any Cu atoms.
3. Because of the anisotropy of the exchange the two R^{3+} ions in the primitive chemical unit cell may couple antiferromagnetically, if the moments are aligned along the a direction, but ferromagnetically, if the moments are aligned along the b direction. Therefore, the ordering wave vector is not the same for all RCu_2 compounds. It is approximately $\mathbf{Q} \sim (2/3\,1\,0)$, if the easy axis is the a or the c axis and $\mathbf{Q} \sim (2/3\,0\,0)$ if b is the easy axis.

We appreciate the fruitful discussions with A. Lindbaum, M. Ellerby, A. Metz and J. Jensen concerning the theoretical part of this work. Some of us (S.K. and M.R.) would like to acknowledge the support of the Hahn–Meitner–Institut (PECO). Part of this work was supported by the Austrian science foundation (FWF) project No 11239-PHY, the single crystal has been financed by the FWF project No 8913-PHY. Part of this work was performed within the program of the Sonderforschungsbereich 463 (funded by the Deutsche Forschungsgemeinschaft). We acknowledge funding of IN12 experiments by the German Research Ministry BMBF under project No. 05-300-CJB-6.

Appendix A

Here a more quantitative argument for the importance of anisotropic exchange in $NdCu_2$ will be presented. It is based on the analysis of the magnetic structures of this compound [3]. Figure 10 shows the free energy of the different magnetic structures in a magnetic field parallel to the b-direction. For every magnetic structure the free energy at zero temperature is given by a line, the slope of which is determined by the total magnetic moment of the

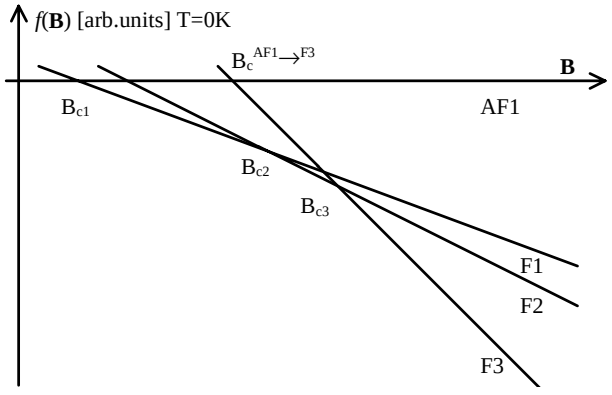

Fig. 10. Model: Magnetic free energy f at zero temperature as a function of the magnetic field B for the different structures AF1, F1, F2, F3 (neglecting the contribution of higher CF levels).

structure. The position of the line is determined by the special moment arrangement of this structure [3]. Therefore, if the magnetic structure and the transition fields B_{c1}, B_{c2} and B_{c3} are known from experiment, the position of all lines in Figure 10 can be determined (see [3]). Also the value of the critical field B_c^{AF1-F3} can be calculated, although this critical field cannot be observed directly in experiments. Thus the value of B_c^{AF1-F3} has been determined to 1.965 T [3]. At this field the free energy of F3 equals the free energy of AF1 and this fact may be used to make important conclusions about the magnetic exchange in this compound.

We will assume that the exchange is isotropic and show that this leads to contradictions with the experimentally observed magnitude of the excitation energy within the mean field (MF) – random phase approximation (RPA) model.

The magnetic energy of the zero field phase AF1 (per formula unit) can be calculated directly from the exchange interaction

$$f_{\rm AF1} = -\frac{1}{2N}\sum_{i,j}\langle \mathbf{J}_i\rangle_{\rm AF1}\overline{\overline{\mathcal{J}}}(ij)\langle \mathbf{J}_j\rangle_{\rm AF1}. \qquad (A.1)$$

In this expression the $\overline{\overline{\mathcal{J}}}(ij)$ represents the exchange tensors between Nd ion number i and j (at position $\mathbf{R}_i$ and

$\mathbf{R}_j$) and the $< \mathbf{J}_i >_{\mathrm{AF1}}$ represent the thermal expectation values of the angular momentum operator for the special spin configuration of AF1 in a crystal of N Nd-atoms.

For $\mathbf{q} \perp \mathbf{c}$ equation (A.1) can be Fourier transformed to give

$$f_{\mathrm{AF1}} = -\frac{1}{2} \sum_{\mathbf{q}\perp\mathbf{c}\in 1.\mathrm{BZ}} \langle \mathbf{J}(-\mathbf{q})\rangle_{\mathrm{AF1}} \overline{\overline{\mathcal{J}}}(\mathbf{q}) \langle \mathbf{J}(\mathbf{q})\rangle_{\mathrm{AF1}} \quad \text{(A.2)}$$

with the Fourier transform of the exchange and the spin arrangement defined as

$$\overline{\overline{\mathcal{J}}}(\mathbf{q}) = \sum_j \overline{\overline{\mathcal{J}}}(ij) \exp[-\mathrm{i}\mathbf{q}(\mathbf{R}_i - \mathbf{R}_j)] \quad \text{(A.3)}$$

$$\langle \mathbf{J}(\mathbf{q})\rangle_{\mathrm{AF1}} = \frac{1}{N} \sum_j \langle \mathbf{J}_j\rangle_{\mathrm{AF1}} \exp(-\mathrm{i}\mathbf{q}\mathbf{R}_j). \quad \text{(A.4)}$$

At zero temperature the expectation values in equation (A.3) ($\langle \mathbf{J}_j\rangle_{\mathrm{AF1}} = \pm M\hat{\mathbf{b}}$, the sign depending on j) can be evaluated from the magnetic structure of AF1 (collinear antiferromagnetic stacking of ferromagnetic bc-planes with the moment arrangement ↑↑↓↓↑↓↓↑↑↓). Then equation (A.2) simply reads

$$f_{\mathrm{AF1}} = -M^2 \Big\{ \mathcal{J}^{bb}(\boldsymbol{\tau})(0.647)^2 + \mathcal{J}^{bb}(3\boldsymbol{\tau})(0.247)^2 + \frac{1}{2}\mathcal{J}^{bb}(5\boldsymbol{\tau})(0.200)^2 \Big\}. \quad \text{(A.5)}$$

Here $\boldsymbol{\tau}$ =(0.6 0 0) designates the ordering wave vector of AF1. The factor 1/2 for the higher harmonic $5\boldsymbol{\tau}$ results from the fact that the zone boundaries have to be counted only half in the expansion (A.2).

For the free energy of the ferromagnetic phase F3 the total magnetic moment is not zero. In an external magnetic field B oriented parallel to the b-direction the Zeeman energy has to be considered in addition to the exchange interaction, yielding:

$$f_{\mathrm{F3}} = -g_{\mathrm{J}}\mu_{\mathrm{B}} MB - \mathcal{J}^{bb}(\mathbf{q}=0)M^2/2. \quad \text{(A.6)}$$

As stated above the free energies f_{AF1} and f_{F3} are equal at $B_{\mathrm{c}}^{\mathrm{AF1-F3}} = 1.965$ T. This leads to the relation

$$M^2\{\mathcal{J}^{bb}(\boldsymbol{\tau})(0.647)^2 + \mathcal{J}^{bb}(3\boldsymbol{\tau})(0.247)^2 + \frac{1}{2}\mathcal{J}^{bb}(5\boldsymbol{\tau})(0.200)^2\} = g_{\mathrm{J}}\mu_{\mathrm{B}} MB_{\mathrm{c}}^{\mathrm{AF1-F3}} + \mathcal{J}^{bb}(\mathbf{q}=0)M^2/2. \quad \text{(A.7)}$$

To continue the investigation of the exchange, the value of the Néel temperature $T_{\mathrm{N}} = 6.5$ K has to be explained. In a MF theory this is given by (k_{B} denotes Boltzmanns constant)

$$k_{\mathrm{B}}T_{\mathrm{N}} = M^2 \mathcal{J}^{bb}(\boldsymbol{\tau}). \quad \text{(A.8)}$$

The small shift of $\boldsymbol{\tau}$ with temperature [3] has been neglected in this expression. The structure AF1 can only be stable, if the Fourier transform of the exchange $\mathcal{J}^{bb}(\mathbf{q})$ has its maximum at $\mathbf{q} = \boldsymbol{\tau}$ (*i.e.* $\mathcal{J}^{bb}(\boldsymbol{\tau}) > \mathcal{J}^{bb}(3\boldsymbol{\tau})$, $\mathcal{J}^{bb}(\boldsymbol{\tau}) > \mathcal{J}^{bb}(5\boldsymbol{\tau})$) [16]. Replacing in the left side of equation (A.7) the higher harmonics $\mathcal{J}^{bb}(3\boldsymbol{\tau})$ and $\mathcal{J}^{bb}(5\boldsymbol{\tau})$ by $\mathcal{J}^{bb}(\boldsymbol{\tau}) = k_{\mathrm{B}}T_{\mathrm{N}}/M^2$ gives the relation

$$2k_{\mathrm{B}}T_{\mathrm{N}} \left\{ (0.647)^2 + (0.247)^2 + \frac{1}{2}(0.200)^2 \right\} > 2g_{\mathrm{J}}\mu_{\mathrm{B}} MB_{\mathrm{c}}^{\mathrm{AF1-F3}} + \mathcal{J}^{bb}(\mathbf{q}=0)M^2. \quad \text{(A.9)}$$

By inserting reasonable values for $M = 2.54$ (this corresponds to the moment per Nd at 3 T external field – compare [3]), $T_{\mathrm{N}} = 6.5$ K (*i.e.* $\mathcal{J}^{bb}(\boldsymbol{\tau}) = 0.093$ meV) and $B_{\mathrm{c}}^{\mathrm{AF1-F3}} = 1.965$ T an upper limit for the sum of all coupling parameters (*i.e.* $\mathcal{J}^{bb}(\mathbf{q}=0)$) can be deduced:

$$\mathcal{J}^{bb}(\mathbf{q}=0) < 0.0215 \text{ meV}. \quad \text{(A.10)}$$

This may be used to find an upper limit for the splitting of the ground state doublet in F3 at 3 T, which in a MF-theory is given by

$$\Delta = 2g_{\mathrm{J}}\mu_{\mathrm{B}} MB + 2M^2\mathcal{J}^{bb}(\mathbf{q}=0) < 0.214 \text{ meV/T} \times 3\text{T} + 2 \times 0.139 \text{ meV} = 0.920 \text{ meV}. \quad \text{(A.11)}$$

Using equation (18) and specializing it for the case of isotropic exchange ($\mathcal{J}^{aa} = \mathcal{J}^{bb} = \mathcal{J}^{cc} = \mathcal{J}$) allows to estimate the excitation energy of the lower magnetic excitation at the wave vector $\boldsymbol{\tau}$ to (for the derivation of this formula see the main text)

$$[\hbar\omega_2(\boldsymbol{\tau})]^2 = (\Delta - 2A^2\mathcal{J}(\boldsymbol{\tau}))(\Delta + 2C^2\mathcal{J}(\boldsymbol{\tau})). \quad \text{(A.12)}$$

Putting in values for A and C (Ref. [7]: $A = 2.1$, $C = 1.5i$) and estimating again $\mathcal{J}(\boldsymbol{\tau})$ from the Néel temperature gives

$$[\hbar\omega_2(\boldsymbol{\tau})]^2 = (\Delta - 0.76\,\mathrm{meV})(\Delta - 0.39\,\mathrm{meV}). \quad \text{(A.13)}$$

If we compare this to the estimation (A.11) ($\Delta < 0.92$ meV), we can conclude that the soft mode excitation $\hbar\omega_2(\boldsymbol{\tau})$ has to lie below 0.08 meV, which is one order of magnitude lower than the measured excitation energy of about 1 meV. Therefore the assumption of isotropic exchange leads to fundamental contradictions with the experiment.

Note that the numerical values in equations (A.7–A.13) are based on the original analysis of the magnetic phase diagram [3] and are in contrast to the new fitted value of $\mathcal{J}^{bb}(\mathbf{q}=0) = 0.044$ meV and $\Delta = 1.106$ meV described in the main text. The most convincing explanation for this discrepancy is the limited validity of the mean field theory near the ordering temperature. Usually the mean field approach predicts an ordering temperature which is too big in comparison with the experiment. Critical fluctuations reduce this ordering temperature (compare for instance Monte-Carlo calculations on Ising models [22,23]). To account for this effect a bigger value for T_{N} has to be inserted into equation (A.9). Taking for example $T_{\mathrm{N}} = 8$ K leads to $\Delta < 1.184$ meV (instead of (A.11)) and $\hbar\omega_2(\boldsymbol{\tau}) < 0.336$ meV – but also these values rule out the possibility of isotropic exchange.

References

1. R.R. Arons, M. Loewenhaupt, Th. Reif, E. Gratz, J. Phys.-Cond. **6**, 6789 (1994).
2. M. Loewenhaupt, T. Reif, R. Arons, E. Gratz, M. Rotter, B. Lebech, Z. Phys. B **96**, 491 (1995).
3. M. Loewenhaupt, T. Reif, P. Svoboda, S. Wagner, M. Waffenschmidt, H.V. Löhneysen, E. Gratz, M. Rotter, B. Lebech, T. Hauss, Z. Phys. B **101**, 499 (1996).
4. E. Gratz, M. Loewenhaupt, M. Divis, W. Steiner, E. Bauer, N. Pillmayr, H. Müller, H. Novotny, B. Frick, J. Phys.-Cond. **3**, 9297 (1991).
5. M. Loewenhaupt, T. Reif, W. Hahn, B. Frick, J. Magn. Magn. Mat. **177-181**, 1050 (1998).
6. E. Gratz, N. Pillmayr, E. Bauer, H. Müller, B. Barbara, M. Loewenhaupt, J. Phys.-Cond. **2**, 1485 (1990).
7. P. Svoboda, M. Divis, A.V. Andreev, N.V. Baranov, M.I. Bartashevich, P.E. Markin, J. Magn. Magn. Mat. **104-107**, 1329 (1992).
8. A. Loidl, K. Knorr, J.K. Kjems, B. Luethi, Z. Phys. B **35**, 253 (1979).
9. B. Haelg, A. Furrer, Phys. Rev. B **34**, 6258 (1986).
10. J. Jensen, J. Magn. Magn. Mat. **29**, 47 (1982).
11. P. Ahmet, M. Abliz, R. Settai, K. Sugiyama, Y. Onuki, T. Takeuchi, K. Kindo, S. Takayanagi, J. Phys. Soc. Japan **65**, 1077 (1996).
12. Y. Hashimoto, K. Kindo, T. Takeuchi, K. Senda, M. Date, A. Yamagishi, Phys. Rev. Lett. **72**, 1922 (1994).
13. M. Loewenhaupt, M. Doerr, L. Jahn, T. Reif, C. Sierks, M. Rotter, H. Müller, Physica B **246-247**, 472 (1998).
14. T. Reif, Ph.D. thesis, Universität zu Köln (1998).
15. M. Rotter, A. Lindbaum, E. Gratz, H. Müller, G. Hilscher, H. Sassik, H.E. Fischer, M.T. Fernandes-Diaz, R. Arons, E. Seidl, J. Phys.-Cond. (submitted).
16. J. Jensen, A.R. Mackintosh, *Rare Earth Magnetism* (Clarendon Press, Oxford, 1991).
17. K.W.H. Stevens, Proc. Phys. Soc. A **65**, 209 (1952).
18. S. Kirkpatrick, C.D. Gelatt, M.P. Vecchi, Science **220**, 671 (1983).
19. S. Kawarazaki, Y. Kobashi, M. Sato, Y. Miyako, J. Phys.-Cond. **7**, 4051 (1995).
20. K. Poldy, H. Kirchmayer, Phys. Stat. Solidi B **65**, 553 (1974).
21. N. Iwata, Y. Hashimoto, T. Kimura, T. Shigeoka, J. Magn. Magn. Mat. **81**, 354 (1989).
22. W. Selke, M.E. Fisher, Phys. Rev. B **20**, 257 (1979).
23. W. Selke, Z. Phys. B **29**, 133 (1978).
24. V. Sima, Z. Smetana, B. Lebech, E. Gratz, J. Magn. Magn. Mat. **54-57**, 1357 (1986).
25. B. Lebech, Z. Smetana, V. Sima, J. Magn. Magn. Mat. **70**, 97 (1987).
26. Y. Koike, N. Metoki, Y. Morii, Y. Yoshida, R. Settai, Y. Onuki, J. Phys. Soc. Japan **66**, (1997).
27. Z. Smetana, V. Sima, B. Lebech, J. Magn. Magn. Mat. **59**, 145 (1986).
28. Y. Hashimoto, H. Kawano, H. Yoshizawa, S. Kawano, T. Shigeoka, J. Magn. Magn. Mat. **140-144**, 1131 (1995).
29. M. Heidelmann, Ph.D. thesis, Universität zu Köln (1992).
30. R. Trump, Ph.D. thesis, Universität zu Köln (1991).
31. V. Nunez, R. Trump, P.J. Brown, T. Chattopadhyay, M. Loewenhaupt, F. Tasset, J. Phys.-Cond. **4**, 1115 (1992).
32. Y. Hashimoto, J. Sci. Hiroshima Univ. **43**, 157 (1979).
33. R. Settai, S. Araki, P. Ahmet, M. Abliz, K. Sugiyama, Y. Onuki, T. Goto, H. Mitamura, T. Goto, S. Takayanagi, J. Phys. Soc. Japan **67**, 636 (1998).
34. K. Maezawa, S. Wakabayashi, K. Sato, Y. Isikawa, T. Kaneko, G. Kido, Y. Nakagawa, Physica B **155**, 276 (1989).